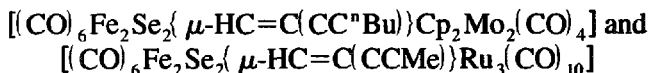


**Diyne-bridged metal clusters: synthesis and spectroscopic characterization of  $[(\text{CO})_6\text{Fe}_2\text{Se}_2\{\mu\text{-HC}=\text{C}(\text{CCR})\}\text{M}]$  ( $\text{R} = \text{Me}$  and  ${}^n\text{Bu}$ ;  $\text{M} = \text{Cp}_2\text{Mo}_2(\text{CO})_4$ ,  $\text{Co}_2(\text{CO})_6$ ,  $\text{Ru}_3(\text{CO})_{10}$  and  $\text{Os}_3(\text{CO})_{10}$ ).**

**Structural characterization of**



Pradeep Mathur <sup>a,\*</sup>, Aswini K. Dash <sup>a</sup>, Md. Munkir Hossain <sup>a</sup>, C.V.V. Satyanarayana <sup>b</sup>, Arnold L. Rheingold <sup>c</sup>, Louise M. Liable-Sands <sup>c</sup>, Glenn P.A. Yap <sup>c</sup>

<sup>a</sup> Chemistry Department, Indian Institute of Technology, Powai, Bombay 400 076, India

<sup>b</sup> Regional Sophisticated Instrumentation Center, Indian Institute of Technology, Powai, Bombay 400 076, India

<sup>c</sup> Department of Chemistry, University of Delaware, Newark, DE 19716, USA

Received 31 July 1996; revised 3 October 1996

**Abstract**

Room temperature reaction of  $[(\text{CO})_6\text{Fe}_2\{\mu\text{-SeC(H)=C(C}\equiv\text{CR)Se}\}]$ , with the dimetallic species,  $\text{Cp}_2\text{Mo}_2(\text{CO})_4$  and  $\text{Co}_2(\text{CO})_6$ , afforded the adducts  $[(\text{CO})_6\text{Fe}_2\text{Se}_2\{\mu\text{-HC}=\text{C}(\text{CCR})\}\text{Cp}_2\text{Mo}_2(\text{CO})_4]$  ( $\text{R} = \text{Me}$ , 1;  $\text{R} = {}^n\text{Bu}$ , 2) and  $[(\text{CO})_6\text{Fe}_2\text{Se}_2\{\mu\text{-HC}=\text{C}(\text{CCR})\}\text{Co}_2(\text{CO})_6]$  ( $\text{R} = \text{Me}$ , 3;  $\text{R} = {}^n\text{Bu}$ , 4) respectively. On reaction of  $\text{Ru}_3(\text{CO})_{10}$  ( $\text{NCMe})_2$  with  $[(\text{CO})_6\text{Fe}_2\{\mu\text{-SeC(H)=C(C}\equiv\text{CR)Se}\}]$ , the new diyne-bridged mixed-metal clusters  $[(\text{CO})_6\text{Fe}_2\text{Se}_2\{\mu\text{-HC}=\text{C}(\text{CCR})\}\text{Ru}_3(\text{CO})_{10}]$  ( $\text{R} = \text{Me}$ , 5;  $\text{R} = {}^n\text{Bu}$ , 6) were obtained. Similarly,  $[(\text{CO})_6\text{Fe}_2\text{Se}_2\{\mu\text{-HC}=\text{C}(\text{CC}^n\text{Bu})\}\text{Os}_3(\text{CO})_{10}]$ , 7, was isolated from the reaction of  $[(\text{CO})_6\text{Fe}_2\{\mu\text{-SeC(H)=C(C}\equiv\text{C}^n\text{Bu)Se}\}]$  with  $\text{Os}_3(\text{CO})_{10}(\text{NCMe})_2$ . Compounds 1–7 were characterized by IR and  ${}^1\text{H}$ ,  ${}^{13}\text{C}$  and  ${}^{77}\text{Se}$  NMR spectroscopy. The structures of 2 and 5 were established by single crystal X-ray diffraction study. Both contain an  $\text{Fe}_2\text{Se}_2$  butterfly core bridged by an HCC unit of the diyne  $\text{HC}\equiv\text{CC}=\text{CR}$  across the two Se atoms. In 2, the substituted acetylenic moiety is transversely bridged to the Mo–Mo bond and in 5, it forms a  $\mu_3\text{-}\eta^2$  bridge to an  $\text{Ru}_3$  triangular core.

**Keywords:** Iron; Molybdenum; Cobalt; Ruthenium; Osmium; Selenium; Carbonyl; Diyne; Crystal structure

**1. Introduction**

The class of compounds  $(\text{CO})_6\text{Fe}_2(\mu\text{-E}_2)$ , ( $\text{E} = \text{S}$ , Se, Te) have been used extensively as starting materials for cluster growth purposes, and for the manipulation of various organic species bonded to the E atoms of these complexes [1]. The nature of E influences strongly the reactivities of  $(\text{CO})_6\text{Fe}_2(\mu\text{-E}_2)$  towards inorganic and organic species [2]. Towards acetylenes, the Se–Se bond appears to be the most reactive, as seen by the

room temperature addition of phenylacetylene to form  $(\text{CO})_6\text{Fe}_2\{\mu\text{-SeC(H)=C(Ph)Se}\}$  and  $[(\text{CO})_6\text{Fe}_2\text{Se}_2\{\mu\text{-C(H)-C(Ph)}\}]$  [3]. The corresponding  $\text{S}_2$  and  $\text{Te}_2$  compounds,  $(\text{CO})_6\text{Fe}_2(\mu\text{-S}_2)$  and  $(\text{CO})_6\text{Fe}_2(\mu\text{-Te}_2)$ , are inert towards such acetylene addition under similar conditions [4]. Phenylacetylene addition serves to block the reactive Se sites of  $(\text{CO})_6\text{Fe}_2(\mu\text{-Se}_2)$  and this enables cluster growth to occur across the Fe–Fe bond. For example, thermolysis of  $(\text{CO})_6\text{Fe}_2\{\mu\text{-SeC(H)=C(Ph)Se}\}$  and  $\text{Cp}_2\text{Mo}_2(\text{CO})_6$  forms the mixed-metal cluster  $\text{Cp}_2\text{Mo}_2\text{Fe}_2(\text{CO})_6(\mu_4\text{-Se})(\mu_3\text{-Se})_2$ , the structure of which consists of an  $\text{Mo}_2\text{Fe}_2$  open butterfly tetrahedron core with the Fe atoms located at the ‘wing-tips’ [5]. Dienes coordinated

\* Corresponding author.

to metal centers have been of interest in recent times [6]. Novel metalacumulenes containing  $R_2C=C=C=Ru=C=C=CR_2$  units have been obtained from derivatives of 1,3-butadiyne [7]. Metal–diyne complexes have also been regarded to be of use for obtaining novel polynuclear complexes [8].

We have previously reported the formation of an Se-bridged complex containing an *s-trans*-1,3-diene ligand [9] and the functionalization of  $MeC\equiv C=CH$  on the mixed-chalcogenide compound  $(CO)_6Fe_2(\mu\text{-}STe)$  [10]. The compounds  $[(CO)_6Fe_2\{\mu\text{-}SeC(H)=C(C=CR)Se\}]$  ( $R = Me, ^nBu$ ) have been obtained by room temperature reaction of  $(CO)_6Fe_2(\mu\text{-}Se_2)$  with  $HC\equiv C=CR$  [11]. The availability of an uncoordinated triple bond in  $(CO)_6Fe_2\{\mu\text{-}SeC(H)=C(C=CMe)Se\}$  has been used for the addition of a trisium carbonyl group and the diyne-bridged mixed-metal complex  $[(CO)_6Fe_2Se_2\{\mu\text{-}HC=C(CCMe)Os_3(CO)_{10}\}]$  has been obtained [11]. In this paper we report on the reaction of  $[(CO)_6Fe_2\{\mu\text{-}SeC(H)=C(C=CR)Se\}]$  ( $R = Me, ^nBu$ ) with  $Cp_2Mo_2(CO)_3$ ,  $Co_2(CO)_8$ , and  $(CO)_9M_1(NCMe)_2$  ( $M = Ru, Os$ ).  $^{77}Se$  NMR of  $[(CO)_6Fe_2\{\mu\text{-}SeC(H)=C(C=CR)Se\}]$  and  $[(CO)_6Fe_2Se_2\{\mu\text{-}HC=C(CCMe)Os_3(CO)_{10}\}]$  are also reported.

## 2. Experimental section

Reactions and manipulations were carried out under an inert atmosphere of nitrogen or argon using standard Schlenk techniques. Solvents were purified and deoxygenated immediately prior to use. Infrared spectra were recorded on a Nicolet Impact 400 Fourier transform spectrometer in NaCl cell of 0.1 mm path length as hexane solutions.  $^1H$ ,  $^{13}C$ , and  $^{77}Se$  spectra were obtained on a Varian VXR-300S spectrometer in  $CDCl_3$  solutions using appropriate references at 25 °C. The  $^{77}Se$  NMR signals were referenced to  $Me_2Se$  ( $\delta = 0$  ppm) and the spectra were obtained at an operating frequency of 57.23 MHz; 90° pulses were used with 2 s delay and 1 s acquisition time. Elemental analyses were carried out using a Carlo Erba automatic analyzer.  $[(CO)_6Fe_2\{\mu\text{-}SeC(H)=C(C=CR)Se\}]$  ( $R = Me, ^nBu$ ) [11],  $Cp_2Mo_2(CO)_3$  [12],  $Ru_3(CO)_9(CH_3CN)_2$  [13] and  $Os_3(CO)_9(CH_3CN)_2$  [14] were prepared as reported previously.  $Co_2(CO)_8$  was purchased from Aldrich Chemicals and sublimed before use.

### 2.1. Reaction of $Cp_2Mo_2(CO)_3$ with $[(CO)_6Fe_2\{\mu\text{-}SeC(H)=C(C=CR)Se\}]$ ( $R = Me, ^nBu$ )

To a dichloromethane solution (30 ml) containing freshly prepared  $Cp_2Mo_2(CO)_3$  (0.57 g, 0.22 mmol) was added  $[(CO)_6Fe_2\{\mu\text{-}SeC(H)=C(C=CMe)Se\}]$  (0.084 g, 0.19 mmol) in 15 ml of benzene and the reaction mix-

ture was stirred at room temperature for 1 h. After removal of the solvent in vacuo, the residue was subjected to chromatographic work-up on silica gel TLC plates. Use of dichloromethane:hexane (1:5 v/v) solution mixture as eluent afforded trace amounts of  $Cp_2Mo_2(CO)_3$  and  $[(CO)_6Fe_2\{\mu\text{-}SeC(H)=C(C=CMe)Se\}]$ , followed by a dark brown band of  $[(CO)_6Fe_2Se_2\{\mu\text{-}HC=C(CCMe)Cp_2Mo_2(CO)_3\}]$  **1** (0.086 g, (65%)). **1**: IR  $\nu(CO)$ : 2067(vs), 2035(m), 2030(vs), 1999(vs), 1989(m), 1977(m), 1964(m), 1939(vs), 1920(m), 1861(sh)  $cm^{-1}$ .  $^1H$  NMR:  $\delta$  2.7 (s,  $CH_3$ ), 5.25 (s,  $C_5H_5$ ), 6.45 (s,  $^2J_{H-Se} = 56$  Hz,  $^3J_{H-Se} = 8$  Hz, CH) ppm;  $^{13}C$  (H) NMR:  $\delta$  25.3 (q,  $J = 130$  Hz,  $CH_3$ ), 92.3 (m,  $C_5H_5$ ), 105.4 (s,  $CCH_2$ ), 113.7 (s,  $C=CCH$ ), 122.4 (d,  $J = 184$  Hz, CH), 135.8 (s,  $C=CH$ ), 210 (s, CO), 227 (s, CO) ppm;  $^{77}Se$  NMR:  $\delta$  372.4 (d,  $J_{Se-H} = 56$  Hz), 465.2 (d,  $J_{Se-H} = 8$  Hz) ppm. M.p. 146 °C (decomp.). Anal. Found: C, 43.0; H, 2.16.  $C_{25}H_{14}Fe_2Mo_2O_{10}Se_2$ . Calc.: C, 42.8; H, 1.99%.

The reaction of  $[(CO)_6Fe_2\{\mu\text{-}SeC(H)=C(C=^nBu)Se\}]$  with  $Cp_2Mo_2(CO)_3$  yielded dark brown  $[(CO)_6Fe_2Se_2\{\mu\text{-}HC=C(C^nBu)Cp_2Mo_2(CO)_3\}]$  **2** in 62% yield after work-up as described for the preparation of **1**. **2**: IR  $\nu(CO)$ : 2067(vs), 2057(m), 2030(vs), 1997(vs), 1976(w), 1965(m), 1937(s), 1920(m), 1860(sh)  $cm^{-1}$ .  $^1H$  NMR:  $\delta$  1.04 (t,  $CH_3$ ), 2.02 (m,  $CH_2$ ), 2.28 (m,  $CH_2$ ), 2.82 (t,  $CH_2$ ), 5.23 (s,  $C_5H_5$ ), 6.45 (s,  $^2J_{H-Se} = 56$  Hz,  $^3J_{H-Se} = 8$  Hz, CH) ppm;  $^{13}C$  (H) NMR:  $\delta$  13.9 (q,  $J = 126$  Hz,  $CH_3$ ), 26.4 (t,  $J = 124$  Hz,  $CH_2CH_3$ ), 38.3 (t,  $J = 127$  Hz,  $CH_2CH_2CH_3$ ), 46.8 (t,  $J = 130$  Hz,  $CH_2CH_2CH_2CH_3$ ), 92.4 (m,  $C_5H_5$ ), 106.9 (s,  $C^nBu$ ), 114.5 (s,  $C\equiv C^nBu$ ), 122.6 (d,  $J = 184$  Hz, CH), 136.1 (s,  $C=CH$ ), 209 (s, CO), 227 (s, CO) ppm;  $^{77}Se$  NMR:  $\delta$  371.0 (d,  $J_{Se-H} = 56$  Hz), 470.6 (d,  $J_{Se-H} = 8$  Hz) ppm. M.p. 152 °C (decomp.). Anal. Found: C, 45.5; H, 2.88.  $C_{25}H_{20}Fe_2Mo_2O_{10}Se_2$ . Calc.: C, 45.2; H, 2.69%.

### 2.2. Reaction of $Co_2(CO)_8$ with $[(CO)_6Fe_2\{\mu\text{-}SeC(H)=C(C=CR)Se\}]$ ( $R = Me, ^nBu$ )

To a hexane solution (30 ml) containing  $[(CO)_6Fe_2\{\mu\text{-}SeC(H)=C(C=CMe)Se\}]$  (0.084 g, 0.19 mmol) was added solid  $Co_2(CO)_8$  (0.071 g, 0.21 mmol) and the reaction mixture was stirred at room temperature for 2 h. The solvent was removed in vacuo and the residue was dissolved in 5 ml of dichloromethane. Chromatographic work-up on silica gel TLC plates using hexane as eluent yielded trace amounts of  $[(CO)_6Fe_2\{\mu\text{-}SeC(H)=C(C=CMe)Se\}]$  and  $Co_2(CO)_8$  followed by dark violet compound  $[(CO)_6Fe_2Se_2\{\mu\text{-}HC=C(CCMe)Co_2(CO)_8\}]$  **3** (0.135 g, (98%)). **3**: IR  $\nu(CO)$ : 2096(s), 2071(vs), 2061(vs), 2038(vs), 2031(m), 2019(m), 2001(vs), 1987(m)  $cm^{-1}$ .  $^1H$  NMR:  $\delta$  2.6 (s,  $CH_3$ ), 7.24 (s,  $^2J_{H-Se} = 53$  Hz,

$^3J_{H-Se} = 6$  Hz, *CH*) ppm;  $^{13}C$ ( $^1H$ ) NMR:  $\delta$  20.8 (q,  $J = 130$  Hz,  $CH_3$ ), 83.5 (s,  $CCH_3$ ), 96.8 (s,  $CCCH_3$ ), 131.2 (d,  $J = 184$  Hz,  $CH$ ), 155.5 (s,  $CCH$ ), 198 (s,  $CO$ ), 209 (s,  $CO$ ) ppm;  $^{77}Se$  NMR:  $\delta$  371.1 (d,  $^2J_{Se-H} = 53$  Hz), 465.6 (d,  $^3J_{Se-H} = 6$  Hz) ppm. M.p. 100–102°C (decomp.). Anal. Found: C, 28.3; H, 0.63.  $C_{19}H_4Co_2Fe_2O_{12}Se_2$ . Calc.: C, 28.1; H, 0.55%.

The reaction of  $[(CO)_6Fe_2\{\mu-SeC(H)=C(C=C^nBu)Se\}]$  with  $Co_2(CO)_8$  yielded dark violet  $[(CO)_8Fe_2Se_2\{\mu-HC=C(C^nBu)\}Co_2(CO)_8]$ , **4**, in 92% yield after work-up as described above. **4**: IR  $\nu(CO)$ : 2095(s), 2070(vs), 2059(vs), 2038(vs), 2029(m), 2017(m), 2000(vs), 1986(m)  $cm^{-1}$ .  $^1H$  NMR:  $\delta$  1.02 (t,  $CH_3$ ), 1.48 (m,  $C H_2 CH_3$ ), 1.6 (m,  $C H_2 CH_2 CH_3$ ), 2.81 (t,  $C H_2 CH_2 CH_2 CH_3$ ), 7.22 (s,  $^2J_{H-Se} = 53$  Hz,  $^3J_{H-Se} = 6$  Hz, *CH*) ppm;  $^{13}C$ ( $^1H$ ) NMR:  $\delta$  13.8 (q,  $J = 125$  Hz,  $CH_3$ ), 22.7 (t,  $J = 132$  Hz,  $CH_2 CH_3$ ), 34.1 (t,  $J = 133$  Hz,  $CH_2 CH_2 CH_3$ ), 34.1 (t,  $J = 136$  Hz,  $CH_2 CH_2 CH_2 CH_3$ ), 94.0 (s,  $C^nBu$ ), 103.2 (s,  $CC^nBu$ ), 130.6 (d,  $J = 185$  Hz, *CH*), 156.2 (s,  $CCH$ ), 198 (s,  $CO$ ), 209 (s,  $CO$ ) ppm;  $^{77}Se$  NMR:  $\delta$  371.4 (d,  $^2J_{Se-H}$

$= 53$  Hz), 472.1 (d,  $^3J_{Se-H} = 6$  Hz) ppm. M.p. 106–108°C (decomp.). Anal. Found: C, 31.5; H, 1.52.  $C_{22}H_{10}Co_2Fe_2O_{12}Se_2$ . Calc.: C, 31.3; H, 1.30%.

### 2.3. Reaction of $Ru_3(CO)_{10}(NCMe)_2$ with $[(CO)_6Fe_2\{\mu-SeC(H)=C(C=C^R)Se\}]$ ( $R = Me, ^nBu$ )

A benzene solution (50 ml) of freshly prepared  $Ru_3(CO)_{10}(NCMe)_2$  (0.16 g, 0.25 mmol) and  $[(CO)_6Fe_2\{\mu-SeC(H)=C(C=CMe)Se\}]$  (0.084 g, 0.19 mmol) in 15 ml of benzene was stirred at room temperature for 1 h. The solvent was evaporated in vacuo, and the residue was dissolved in 5 ml of dichloromethane. Chromatographic work-up on silica gel TLC plates using hexane as eluent yielded a trace amount of  $Ru_3(CO)_{12}$  followed by red  $[(CO)_8Fe_2Se_2\{\mu-HC=C(C^R)Se\}]Ru_3(CO)_{10}$ , **5** (0.083 g, (43%)). **5**: IR  $\nu(CO)$ : 2099(s), 2085(m), 2071(vs), 2067(m), 2055(m), 2036(vs), 2018(m), 2002(vs), 1954(m), 1888(sh)  $cm^{-1}$ .  $^1H$  NMR:  $\delta$  2.29 (s,  $CH_3$ ), 6.39 (s,  $^2J_{H-Se} = 55$  Hz,  $^3J_{H-Se} = 8$  Hz, *CH*)

Table 1  
Crystallographic data for **2** and **5**

	2	5
<i>Crystal parameters</i>		
Formula	$C_{28}H_{20}O_{10}Fe_2Mo_2Se_2$	$C_{21}H_{16}O_{16}Fe_2Ru_3Se_2$
Formula weight	977.9	1085.1
Crystal system	orthorhombic	triclinic
Space group	<i>Pbcn</i>	<i>P</i> $\bar{1}$
<i>a</i> (Å)	27.213(8)	9.020(2)
<i>b</i> (Å)	10.143(3)	12.904(4)
<i>c</i> (Å)	23.390(5)	14.284(5)
$\alpha$ (deg)	—	82.04(3)
$\beta$ (deg)	—	77.60(2)
$\gamma$ (deg)	—	70.46(2)
<i>V</i> (Å <sup>3</sup> )	6456(3)	1526.3(9)
<i>Z</i>	8	2
<i>D</i> <sub>calc</sub> (g cm <sup>-3</sup> )	2.012	2.361
Crystal dimensions (mm <sup>3</sup> )	0.32 × 0.30 × 0.40	0.2 × 0.2 × 0.6
Crystal color	red	dark red
$\mu$ (Mo K $\alpha$ ) (cm <sup>-1</sup> )	39.48	48.33
Temperature (K)	296	298
<i>Data collection</i>		
Diffractometer	Siemens P4	
Monochromator	graphite	
Radiation	Mo K $\alpha$ ( $\lambda = 0.71073$ Å)	
$2\theta$ scan range (deg)	4–50	4–45
Reflections collected	6433	4072
Independent reflections	5682	3891
Independent observed reflections $F_o \geq 5\sigma(F_o)$	3392	2963
<i>Refinement</i> <sup>a</sup>		
<i>R</i> ( <i>F</i> ) (%)	3.92	6.03
<i>R</i> ( <i>wF</i> ) (%)	4.65	7.47
$\Delta/\sigma$ (max)	0.002	0.010
$\Delta\rho$ (e Å <sup>-3</sup> )	0.60	2.07
<i>N</i> <sub>o</sub> / <i>N</i> <sub>t</sub>	8.5	7.5
GOF	1.0	1.53

<sup>a</sup> Quantity minimized =  $\sum w\Delta^2$ ;  $R = \sum \Delta / \sum (F_o)$ ;  $R(w) = \sum \Delta w^{1/2} / \sum (F_o w^{1/2})$ ;  $\Delta = (F_o - F_c)$ .

ppm;  $^{13}\text{C}\{^1\text{H}\}$  NMR:  $\delta$  34.5 (q,  $J = 128.5$  Hz,  $\text{CH}_3$ ), 120.9 (d,  $J = 183$  Hz, CH), 156.5 (s,  $\text{C}=\text{CH}$ ), 163.9 (s,  $\text{CCH}_3$ ), 169.9 (s,  $\text{C}\equiv\text{CCH}_3$ ), 196 (s, CO), 209 (s, CO) ppm;  $^{77}\text{Se}$  NMR:  $\delta$  391.1 (d,  $^2J_{\text{Se-H}} = 55$  Hz), 545.8 (d,  $J_{\text{Se-H}} = 8$  Hz) ppm. M.p. 134–136°C. Anal. Found: C, 24.9; H, 0.58.  $\text{C}_{21}\text{H}_4\text{Fe}_2\text{O}_{16}\text{Ru}_3\text{Se}_2$ . Calc.: C, 24.6; H, 0.39%.

The reaction of  $[(\text{CO})_6\text{Fe}_2\{\mu\text{-SeC(H)=C(C}\equiv\text{C}^n\text{Bu)Se}\}]$  with  $\text{Ru}_3(\text{CO})_{10}(\text{NCMe})_2$  yielded  $[(\text{CO})_6\text{Fe}_2\text{Se}_2\{\mu\text{-HC=C(CCC}^n\text{Bu)Ru}_3(\text{CO})_{10}\}]$ , **6** in 40% yield after work-up as for the preparation of **5**. IR  $\nu(\text{CO})$ : 2097(vs), 2071(s), 2051(vs), 2038(m), 2031(s), 2026(m), 2001(s), 1985(m), 1952(m), 1889(sh)  $\text{cm}^{-1}$ .  $^1\text{H}$  NMR:  $\delta$  0.99 (t,  $\text{CH}_3$ ), 1.75 (m,  $\text{C}_2\text{H}_5$ ), 2.21 (m,  $\text{C}_2\text{H}_5$ ), 2.72 (t,  $\text{C}_2\text{H}_5$ ), 6.39 (s,  $^2J_{\text{H-Se}} = 56$  Hz,  $^3J_{\text{H-Se}} = 8$  Hz, CH) ppm;  $^{13}\text{C}\{^1\text{H}\}$  NMR:  $\delta$  14.1 (q,  $J = 126$  Hz,  $\text{CH}_3$ ), 22.8 (t,  $J = 124$  Hz,  $\text{CH}_2\text{CH}_3$ ), 35.2 (t,  $J = 125$  Hz,  $\text{CH}_2\text{CH}_2\text{CH}_3$ ), 48.0 (t,  $J = 128$  Hz,  $\text{CH}_2\text{CH}_2\text{CH}_2\text{CH}_3$ ), 120.9 (d,  $J = 183$  Hz, CH), 156.2 (s,  $\text{C}=\text{CH}$ ), 164.42 (s,  $\text{C}^n\text{Bu}$ ), 176.2 (s,  $\text{C}\equiv\text{C}^n\text{Bu}$ ), 196 (s, CO), 209 (s, CO) ppm;  $^{77}\text{Se}$  NMR:  $\delta$  389.6 (d,  $^2J_{\text{Se-H}} = 56$  Hz), 562.9 (d,  $^3J_{\text{Se-H}} = 8$  Hz) ppm. M.p. 126–128°C. Anal. Found: C, 27.4; H, 1.14.  $\text{C}_{23}\text{H}_{10}\text{Fe}_2\text{O}_{16}\text{Ru}_3\text{Se}_2$ . Calc.: C, 27.0; H, 0.94%.

#### 2.4. Reaction of $\text{Os}_3(\text{CO})_{10}(\text{NCMe})_2$ with $[(\text{CO})_6\text{Fe}_2\{\mu\text{-SeC(H)=C(C}\equiv\text{C}^n\text{Bu)Se}\}]$

To a solution of freshly prepared  $\text{Os}_3(\text{CO})_{10}(\text{NCMe})_2$  (0.21 g, 0.25 mmol) in benzene (50 ml) was added  $[(\text{CO})_6\text{Fe}_2\{\mu\text{-SeC(H)=C(C}\equiv\text{C}^n\text{Bu)Se}\}]$  (0.092 g, 0.19 mmol) in 15 ml of benzene. The mixture was stirred at room temperature for 8 h. After removal of the solvent, the residue was dissolved in 5 ml of

Table 2  
Selected bond distances and bond angles for **2**

Bond distances (Å)			
Fe(1)–Se(1)	2.380(2)	Mo(1)–C(9)	2.140(7)
Fe(1)–Se(2)	2.377(2)	Mo(1)–C(10)	2.239(8)
Fe(2)–Se(1)	2.376(2)	Mo(2)–C(9)	2.205(7)
Fe(2)–Se(2)	2.375(2)	Mo(2)–C(10)	2.140(7)
Fe(1)–Fe(2)	2.515(2)	Mo(1)–Mo(2)	2.930(1)
Se(1)–C(7)	1.917(8)	C(8)–C(9)	1.463(10)
Se(2)–C(8)	1.982(7)	C(9)–C(10)	1.346(10)
C(7)–C(8)	1.311(11)	C(16)–O(16)	1.130(11)
Bond angles (deg)			
Fe(1)–Se(1)–Fe(2)	63.9(1)	Mo(1)–C(9)–Mo(2)	84.8(3)
Fe(1)–Se(2)–Fe(2)	63.9(1)	Mo(1)–C(10)–Mo(2)	84.0(3)
Fe(2)–Fe(1)–Se(1)	58.0(1)	Mo(2)–Mo(1)–C(9)	48.5(2)
Fe(2)–Fe(1)–Se(2)	58.0(1)	Mo(2)–Mo(1)–C(10)	46.6(2)
Se(1)–Fe(1)–Se(2)	81.2(1)	C(9)–Mo(1)–C(10)	35.7(3)
Fe(1)–Fe(2)–Se(1)	58.1(1)	Mo(1)–Mo(2)–C(9)	46.7(2)
Fe(1)–Fe(2)–Se(2)	58.1(1)	Mo(1)–Mo(2)–C(10)	49.5(2)
Se(1)–Fe(2)–Se(2)	81.3(1)	C(9)–Mo(2)–C(10)	36.1(3)
Se(1)–C(7)–C(8)	119.5(6)	C(7)–C(8)–C(9)	131.5(7)
Se(2)–C(8)–C(7)	114.9(6)	C(8)–C(9)–C(10)	136.4(7)

Table 3  
Selected bond distances and bond angles for **5**

Bond distances (Å)			
Fe(1)–Se(1)	2.380(3)	Ru(1)–C(18)	2.223(12)
Fe(1)–Se(2)	2.389(3)	Ru(1)–C(19)	2.258(12)
Fe(2)–Se(1)	2.362(2)	Ru(2)–C(18)	2.088(12)
Fe(2)–Se(2)	2.394(2)	Ru(3)–C(19)	2.111(11)
Fe(1)–Fe(2)	2.515(3)	Ru(1)–Ru(2)	2.732(2)
Se(1)–C(20)	1.971(13)	Ru(1)–Ru(3)	2.725(2)
Se(2)–C(21)	1.937(14)	Ru(2)–Ru(3)	2.833(2)
C(18)–C(19)	1.372(22)	C(19)–C(20)	1.454(18)
C(20)–C(21)	1.298(18)	C(10)–O(10)	1.125(26)
Bond Angles (°)			
Fe(1)–Se(1)–Fe(2)	64.1(1)	Ru(2)–Ru(1)–Ru(3)	62.5(1)
Fe(1)–Se(2)–Fe(2)	63.4(1)	Ru(2)–Ru(1)–C(18)	48.5(3)
Fe(2)–Fe(1)–Se(1)	57.6(1)	Ru(2)–Ru(1)–C(19)	70.0(3)
Fe(2)–Fe(1)–Se(2)	58.4(1)	Ru(3)–Ru(1)–C(18)	70.1(3)
Se(1)–Fe(1)–Se(2)	81.1(1)	Ru(3)–Ru(1)–C(19)	49.0(3)
Fe(1)–Fe(2)–Se(1)	58.3(1)	C(18)–Ru(1)–C(19)	35.6(5)
Fe(1)–Fe(2)–Se(2)	58.2(1)	Ru(1)–Ru(2)–Ru(3)	58.6(1)
Se(1)–Fe(2)–Se(2)	81.3(1)	Ru(1)–Ru(2)–C(18)	52.9(3)
Se(1)–C(20)–C(21)	115.6(10)	Ru(3)–Ru(2)–C(18)	69.5(4)
Se(2)–C(21)–C(20)	119.3(10)	Ru(1)–Ru(3)–C(19)	58.9(1)
Ru(2)–C(13)–Ru(3)	81.5(1)	Ru(1)–Ru(3)–C(19)	53.9(3)
Ru(1)–C(18)–Ru(2)	78.6(4)	Ru(2)–Ru(3)–C(19)	69.7(4)
Ru(1)–C(18)–C(19)	73.6(7)	Ru(1)–C(19)–Ru(3)	77.1(4)
Ru(2)–C(18)–C(19)	111.5(8)	Ru(1)–C(19)–C(18)	70.8(7)
Ru(3)–C(19)–C(18)	109.2(8)	C(17)–C(18)–C(19)	122.5(12)
C(18)–C(19)–C(20)	124.9(11)		

dichloromethane. Chromatographic work-up on silica gel TLC plates using hexane as eluent gave a trace amount of  $\text{Os}_3(\text{CO})_{12}$  followed by orange  $[(\text{CO})_6\text{Fe}_2\text{Se}_2\{\mu\text{-HC=C(CCC}^n\text{Bu)Os}_3(\text{CO})_{10}\}]$  (**7**) (0.096 g, (38%)). **7**: IR  $\nu(\text{CO})$ : 2101(vs), 2071(m), 2066(s), 2056(s), 2037(m), 2028(s), 2011(m), 2002(vs), 1996(m), 1984(m), 1970(m) 1954(m), 1855(sh)  $\text{cm}^{-1}$ .  $^1\text{H}$  NMR:  $\delta$  0.98 (t,  $\text{CH}_3$ ), 1.76 (m,  $\text{C}_2\text{H}_5$ ), 2.14 (m,  $\text{C}_2\text{H}_5$ ), 2.78 (t,  $\text{C}_2\text{H}_5$ ), 6.37 (s,  $^2J_{\text{H-Se}} = 56$  Hz,  $^3J_{\text{H-Se}} = 8$  Hz, CH) ppm;  $^{13}\text{C}\{^1\text{H}\}$  NMR:  $\delta$  14.1 (q,  $J = 126$  Hz,  $\text{CH}_3$ ), 22.6 (t,  $J = 124$  Hz,  $\text{CH}_2\text{CH}_3$ ), 35.5 (t,  $J = 129.5$  Hz,  $\text{CH}_2\text{CH}_2\text{CH}_3$ ), 49.9 (t,  $J = 126$  Hz,  $\text{CH}_2\text{CH}_2\text{CH}_2\text{CH}_3$ ), 121.6 (d,  $J = 184$  Hz, CH), 132.7 (s,  $\text{C}=\text{CH}$ ), 157.6 (s,  $\text{C}^n\text{Bu}$ ), 167.9 (s,  $\text{C}\equiv\text{C}^n\text{Bu}$ ), 175 (s, CO) 209 (s, CO) ppm;  $^{77}\text{Se}$  NMR:  $\delta$  386.8 (d,  $^2J_{\text{Se-H}} = 56$  Hz), 550.5 (d,  $^3J_{\text{Se-H}} = 8$  Hz). M.p. 118–120°C. Anal. Found: C, 21.8; H, 0.92.  $\text{C}_{24}\text{H}_{10}\text{Fe}_2\text{O}_{16}\text{Os}_3\text{Se}_2$ . Calc.: C, 21.6; H, 0.75%.

#### 2.5. Crystal structure determination of $[(\text{CO})_6\text{Fe}_2\text{Se}_2\{\mu\text{-HC=C(CCC}^n\text{Bu)Cp}_2\text{Mo}_2(\text{CO})_4\}]$ , **2**, and $[(\text{CO})_6\text{Fe}_2\text{Se}_2\{\mu\text{-HC=C(CCC}^n\text{Me)Ru}_3(\text{CO})_{10}\}]$ , **5**

Suitable crystals for single-crystal X-ray diffraction were selected and mounted with epoxy cement on thin glass fibers. The unit cell parameters were obtained by the least squares refinement of the angular setting of 24 reflections ( $20 < 2\theta < 25^\circ$ ). Crystallographic data are summarized in Table 1.

The photographic data, unit-cell parameters, occurrences of equivalent reflections data for **2** are uniquely consistent for orthorhombic space group *Pbcn*. No evidence of symmetry higher than triclinic was observed for **5** and the *E*-statistics strongly suggested the centrosymmetric space group *P1̄*. The maximum in the final difference map at  $2.07 \text{ e } \text{Å}^{-3}$  is located  $1.11 \text{ Å}$  from Ru(3) and has no chemical significance. The data were corrected for absorption by semi-empirical methods. The space group choices were verified by chemically reasonable results of refinement. The structures

Table 4  
Atomic coordinates ( $\times 10^3$ ) and equivalent isotropic displacement coefficients ( $\text{Å}^2 \times 10^3$ ) for **2**

	<i>x</i>	<i>y</i>	<i>z</i>	$U_{\text{eq}}^a$
Mo(1)	5967.3(3)	8803.1(7)	202.3(3)	32(1)
Mo(2)	6505.8(2)	6329.9(7)	39.5(3)	31(1)
Se(1)	7207.7(3)	8339(1)	2257.2(3)	44(1)
Se(2)	9095(3)	8317.5(9)	1957.9(3)	36(1)
Fe(1)	6575.1(1)	9911(1)	2450.9(5)	42(1)
Fe(2)	6515.6(4)	7559(1)	2784.3(3)	38(1)
O(1)	7185(3)	11069(8)	3356(3)	88(3)
O(2)	5690(3)	10984(9)	2991(3)	104(4)
O(3)	6765(3)	11763(8)	1515(3)	88(4)
O(4)	6621(3)	4721(8)	2599(4)	93(4)
O(5)	7081(3)	7970(6)	3832(3)	58(3)
O(6)	5584(3)	7432(9)	3413(3)	93(4)
O(15)	5095(2)	7350(8)	-372(3)	77(3)
O(16)	5159(2)	9608(7)	1081(3)	67(3)
O(27)	7004(3)	4632(7)	1001(3)	75(3)
O(28)	7484(3)	7929(7)	91(3)	65(3)
C(1)	6946(4)	10620(10)	2993(4)	59(4)
C(2)	6027(4)	10572(10)	2768(4)	62(4)
C(3)	6676(4)	11065(10)	1878(4)	58(4)
C(4)	6587(4)	5819(11)	2664(4)	55(4)
C(5)	6586(3)	7778(9)	3430(4)	46(3)
C(6)	5951(3)	7487(9)	3173(4)	47(3)
C(7)	7026(3)	7820(8)	1496(3)	36(3)
C(8)	6562(3)	7820(7)	1345(3)	27(2)
C(9)	6324(3)	7521(8)	799(3)	28(3)
C(10)	5931(3)	6825(8)	625(3)	30(2)
C(11)	5523(3)	6110(9)	912(4)	46(3)
C(12)	5702(3)	4897(10)	1229(4)	56(4)
C(13)	5298(4)	4287(11)	1597(5)	79(5)
C(14)	5454(5)	2997(14)	1834(6)	125(8)
C(15)	5423(3)	7892(9)	-168(4)	51(3)
C(16)	5462(3)	9258(9)	787(4)	44(3)
C(17)	5863(4)	10883(9)	-164(4)	60(4)
C(18)	6196(4)	10999(9)	305(4)	56(4)
C(19)	6623(4)	10322(9)	159(4)	59(4)
C(20)	6563(4)	9794(9)	-389(4)	57(4)
C(21)	6098(4)	10137(10)	-584(4)	60(4)
C(22)	6133(4)	6130(11)	-872(4)	55(4)
C(23)	5982(3)	5074(11)	-543(4)	59(4)
C(24)	6398(4)	4319(9)	-413(4)	59(4)
C(25)	6806(4)	4914(10)	-643(4)	55(4)
C(26)	6643(4)	6036(10)	-935(4)	54(4)
C(27)	6811(3)	5253(9)	655(4)	46(3)
C(28)	7120(3)	7382(9)	82(3)	40(3)

<sup>a</sup> Equivalent isotropic *U* defined as one-third of the trace of the orthogonalized  $U_{ij}$  tensor.

Table 5

Atomic coordinates ( $\times 10^3$ ) and equivalent isotropic displacement coefficients ( $\text{Å}^2 \times 10^3$ ) for **5**

	<i>x</i>	<i>y</i>	<i>z</i>	$U_{\text{eq}}^a$
Ru(1)	6626(1)	3053.2(9)	1710.5(8)	35(1)
Ru(2)	6340(1)	3016(1)	3657.2(8)	40(1)
Ru(3)	4434(1)	2168.5(9)	2832.8(8)	35(1)
Se(1)	7176(2)	-927(1)	2816.4(9)	32(1)
Se(2)	8797(2)	-1476(1)	722.2(9)	35(1)
Fe(1)	6690(2)	-2013(2)	1770(1)	32(1)
Fe(2)	9382(2)	-2430(2)	2226(1)	35(1)
O(2)	3951(16)	-437(11)	995(10)	80(6)
O(3)	5088(15)	-3092(10)	3414(8)	69(6)
O(4)	12025(15)	-1726(12)	2472(9)	82(7)
O(5)	11052(15)	-4484(10)	1272(10)	80(6)
O(6)	8944(16)	-3613(11)	4122(8)	80(6)
O(7)	6521(16)	2554(10)	-273(8)	72(6)
O(8)	9741(15)	3573(11)	905(9)	77(6)
O(9)	4242(15)	5385(10)	1630(12)	94(7)
O(10)	8061(16)	4696(11)	2912(9)	84(7)
O(11)	3492(17)	4923(12)	4571(11)	96(7)
O(1)	7302(14)	-3894(10)	658(8)	66(6)
O(12)	8414(22)	2123(17)	5193(11)	138(11)
O(13)	4653(18)	1516(12)	5015(8)	91(8)
O(14)	1387(17)	4105(13)	3396(11)	113(8)
O(15)	3014(15)	348(12)	3750(10)	91(7)
O(16)	3437(16)	2065(11)	978(9)	78(9)
C(1)	7057(17)	-3171(13)	1087(10)	44(6)
C(2)	4997(19)	-1051(13)	1299(11)	49(6)
C(3)	5679(18)	-2659(14)	2763(11)	49(7)
C(4)	11012(18)	-2010(13)	2365(10)	47(7)
C(5)	10374(17)	-3671(14)	1640(11)	49(7)
C(6)	9120(18)	-3154(12)	3374(12)	49(7)
C(7)	6541(19)	2745(12)	466(11)	47(7)
C(8)	8603(21)	3379(12)	1186(11)	52(7)
C(9)	5124(19)	4525(14)	1644(12)	56(8)
C(10)	7435(19)	4053(14)	3104(12)	55(7)
C(11)	4536(22)	4257(15)	4264(12)	61(8)
C(12)	7627(22)	2482(16)	4651(13)	70(9)
C(13)	5016(18)	2014(14)	4329(11)	48(7)
C(14)	2473(20)	3385(15)	3196(13)	61(8)
C(15)	3615(17)	994(14)	3421(11)	51(7)
C(16)	3841(18)	2104(12)	1629(12)	46(7)
C(17)	9602(26)	1239(13)	2699(11)	50(7)
C(18)	7782(14)	1768(10)	2767(9)	31(5)
C(19)	6883(14)	1325(10)	2380(8)	22(4)
C(20)	7498(15)	303(10)	1901(9)	31(5)
C(21)	8191(16)	42(11)	1032(10)	37(6)

<sup>a</sup> Equivalent isotropic *U* defined as one-third of the trace of the orthogonalized  $U_{ij}$  tensor.

were solved by direct methods, completed by subsequent difference Fourier syntheses and refined by full-matrix least squares procedures. Molybdenum, ruthenium, iron, and selenium atoms were refined with anisotropic displacement parameters. Carbon and oxygen atoms were refined anisotropically. Hydrogen atoms were treated as idealized contributions. The largest remaining peak in the difference map of  $5 (2.1 \text{ e } \text{Å}^{-3})$  was located in a chemically unreasonable position and was considered as noise.

All software and sources of scattering factors are contained in the SHELXTL PLUS (4.2) or SHELXTL (5.1) program libraries [15]. Tables 2 and 3 list the selected bond distances and bond angles for **2** and **5** respectively. The atom coordinates and isotropic displacement coefficients for **2** and **5** are listed in Tables 4 and 5 respectively.

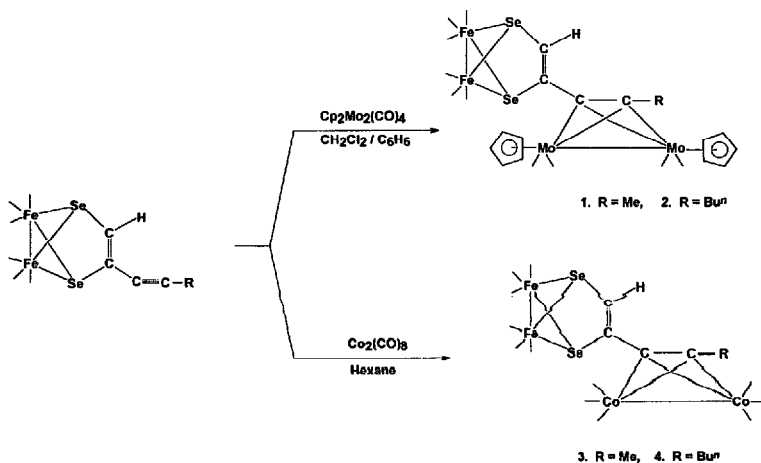
### 3. Results and discussion

#### 3.1. Synthesis and spectroscopic characterization of $[(CO)_6Fe_2Se_2\{\mu-HC=C(CCR)\}M]$ ( $R = Me, {}^nBu; M = Cp_2Mo_2(CO)_4$ or $Co_2(CO)_8$ )

The room temperature reaction of  $[(CO)_6Fe_2\{\mu-SeC(H)=C(C=CR)Se\}]$  ( $R = Me, {}^nBu$ ) with  $Cp_2Mo_2(CO)_4$  in dichloromethane–benzene solvent mixture yielded the adducts  $[(CO)_6Fe_2Se_2\{\mu-HC=C(CCR)\}Cp_2Mo_2(CO)_4]$  (**1**,  $R = Me$ , 65%; **2**,  $R = {}^nBu$ , 62%) (Scheme 1). Clusters **1** and **2** were characterized by IR and  $^1H$ ,  $^{13}C$  and  $^{77}Se$  NMR spectroscopy, and their compositions were confirmed by elemental analysis. The solution IR spectra of **1** and **2** show an almost identical stretching pattern in the terminal carbonyl region.  $^1H$  and  $^{13}C\{^1H\}$  NMR spectra confirm the presence of  $HC_nR$  groups. Short-range (56 Hz) and long-range (8 Hz) H–Se couplings are within the ranges

observed previously in complexes of the form  $[(CO)_6Fe_2\{\mu-SeC(H)=C(Ph)E\}]$  and  $[(CO)_6Fe_2\{\mu-EC(H)=C(Ph)Se\}]$  ( $E = S, Se, Te$ ) (short-range  $J_{H-Se} = 50\text{--}60$  Hz, long-range  $J_{H-Se} = 7\text{--}9$  Hz).  $^{77}Se$  NMR spectra of **1** and **2** (Table 6) show two signals each, in the range observed in complexes containing the  $Fe_2(\mu_3-Se)C$  moieties [16].

Room temperature reactions of  $[(CO)_6Fe_2\{\mu-SeC(H)=C(C=CR)Se\}]$  with  $Co_2(CO)_8$  in hexane solvent afforded the clusters  $[(CO)_6Fe_2Se_2\{\mu-HC=C(CCR)\}Co_2(CO)_8]$  (**3**,  $R = Me$ , 98%; **4**,  $R = {}^nBu$ , 92%) (Scheme 1). The IR spectra of **3** and **4** display peaks due to terminal carbonyl groups and the  $^1H$  and  $^{13}C\{^1H\}$  NMR spectra confirm the presence of  $HC_nMe$  and  $HC_n{}^nBu$  groups in the two clusters respectively.  $^{77}Se$  NMR spectra show two signals for each cluster and each signal is split into a doublet due to Se–H coupling. On the basis of the  $J_{Se-H}$  values, the high field signal is assigned to the Se atom which is attached to  $=CH$  group and the low field signal to the one which is bonded to the  $=C-CR$  group. The chemical shifts of the signals in **3** and **4** show little variation from those in **1** and **2**. In all four compounds, the signal due to the Se atom attached to the CH group is found to shift downfield by 12–14 ppm, whereas the signal due to the Se atom further away from the CH group is found to shift upfield by 48–52 ppm relative to the chemical shift of the Se signals in  $[(CO)_6Fe_2\{\mu-SeC(H)=C(C=CR)Se\}]$ .



Scheme 1. Formation of  $[(CO)_6Fe_2Se_2\{\mu-HC=C(CCR)\}M]$  ( $R = Me$  or  ${}^nBu$ ;  $M = Cp_2Mo_2(CO)_4$  or  $Co_2(CO)_8$ ).

Table 6  
<sup>13</sup>C NMR data for [(CO)<sub>6</sub>Fe<sub>2</sub>Se<sub>2</sub>{μ-C(H)=C(CCR)<sup>n</sup>M}]

M	Two bond distance w.r.t. CH		Three bond distance w.r.t. CH		Two bond distance w.r.t. CH		Three bond distance w.r.t. CH	
	d, δ	<sup>2</sup> J <sub>Se-H</sub>	d, δ	<sup>2</sup> J <sub>Se-H</sub>	d, δ	<sup>2</sup> J <sub>Se-H</sub>	d, δ	<sup>2</sup> J <sub>Se-H</sub>
Nil	δ 358.4 ppm	53 Hz	qd, δ 517.2 ppm	6 Hz	δ 358.9 ppm	53 Hz	td, δ 520.6 ppm	6 Hz
				3 Hz				3 Hz
Cp <sub>2</sub> Mo <sub>2</sub> (CO) <sub>4</sub>	δ 372.4 ppm	56 Hz	δ 465.2 ppm	8 Hz	δ 371.0 ppm	56 Hz	δ 470.6 ppm	8 Hz
Co <sub>2</sub> (CO) <sub>8</sub>	δ 371.1 ppm	53 Hz	δ 465.6 ppm	6 Hz	δ 371.4 ppm	53 Hz	δ 472.1 ppm	6 Hz
Ru <sub>2</sub> (CO) <sub>10</sub>	δ 391.1 ppm	55 Hz	δ 545.8 ppm	8 Hz	δ 389.6 ppm	56 Hz	δ 562.9 ppm	8 Hz
Os <sub>2</sub> (CO) <sub>10</sub>	δ 389.9 ppm	55 Hz	δ 535.3 ppm	7 Hz	δ 386.8 ppm	56 Hz	δ 550.5 ppm	8 Hz

### 3.2. Molecular structure of [(CO)<sub>6</sub>Fe<sub>2</sub>Se<sub>2</sub>{μ-HC=C(CCC<sup>n</sup>Bu)}]Cp<sub>2</sub>Mo<sub>2</sub>(CO)<sub>4</sub> 2

Red colored, air-stable single crystals of **2** were grown from its hexane-dichloromethane solution at -10°C and an X-ray diffraction study was undertaken. An ORTEP diagram of the molecular structure of **2** is shown in Fig. 1. The structure of **2** can be described as consisting of an Fe<sub>2</sub>Se<sub>2</sub> butterfly core, whose wing-tip Se atoms are bonded to the HCC unit of the diyne

ligand HC≡CC≡C<sup>n</sup>Bu, and the substituted acetylenic moiety of the diyne is bonded transversely with respect to the Mo-Mo bond, forming a dimetallatetrahedrane-type Mo<sub>2</sub>C<sub>2</sub> core. Overall, half of the diyne ligand is bridged by the Fe<sub>2</sub>Se<sub>2</sub> butterfly core and the other half by the Mo<sub>2</sub> core. The bond parameters of the (CO)<sub>6</sub>Fe<sub>2</sub>Se<sub>2</sub> butterfly core in **2** are almost identical to those in [(CO)<sub>6</sub>Fe<sub>2</sub>{μ-SeC(H)=C(C≡CMe)<sub>2</sub>Se}] [11]. The C(7)-C(8) bond distance of 1.311(11) Å indicates an olefinic bond order. The Mo-Mo bond distance of 2.930(1) Å in **2** is shorter than 3.267(6) Å in Cp<sub>2</sub>Mo<sub>2</sub>(CO)<sub>4</sub> [17]. It is similar to the corresponding bond distances in complexes containing an Mo<sub>2</sub>C<sub>2</sub> core: Cp<sub>2</sub>Mo<sub>2</sub>(CO)<sub>4</sub>(μ-HC<sub>2</sub>H) (2.180(1) Å) [18], Cp<sub>2</sub>Mo<sub>2</sub>(CO)<sub>4</sub>(μ-EtC<sub>2</sub>Et) (2.977(1) Å) [19], Cp<sub>2</sub>Mo<sub>2</sub>(CO)<sub>4</sub>(μ-PhC<sub>2</sub>Ph) (2.956(1) Å) [20], Cp<sub>2</sub>Mo<sub>2</sub>(CO)<sub>4</sub>(μ-Me<sub>2</sub>SiC<sub>2</sub>SiMe<sub>2</sub>) (2.952(1) Å) [21], (Cp<sub>2</sub>Mo<sub>2</sub>(CO)<sub>4</sub>(μ-HC<sub>2</sub>CH<sub>2</sub>)<sub>2</sub>) (2.981(1) Å) [22], Cp<sub>2</sub>Mo<sub>2</sub>(CO)<sub>4</sub>(μ-Cp(CO)<sub>2</sub>FeC<sub>2</sub>H) (2.972(1) Å) [23], Cp<sub>2</sub>Mo<sub>2</sub>(CO)<sub>4</sub>(μ-(Me<sub>2</sub>SiC<sub>5</sub>H<sub>2</sub>)(CO)<sub>2</sub>FeC<sub>2</sub>H) (2.984(1) Å) [23] and cationic complex Cp<sub>2</sub>Mo<sub>2</sub>(CO)<sub>4</sub>(μ-HC<sub>2</sub>CH<sub>2</sub>PEt<sub>3</sub>)<sup>+</sup> (2.9570(8) Å) [24]. The C(9)-C(10) and Mo(2)-C(10) bond distances in the tetrahedral Mo<sub>2</sub>C<sub>2</sub> core of compound **2** are equal but are shorter than Mo(1)-C(10) (2.239(8) Å) and

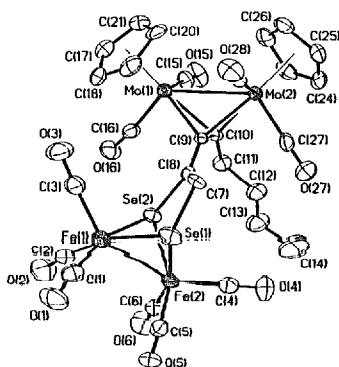


Fig. 1. Molecular structure of [(CO)<sub>6</sub>Fe<sub>2</sub>Se<sub>2</sub>{μ-HC=C(CCC<sup>n</sup>Bu)}]Cp<sub>2</sub>Mo<sub>2</sub>(CO)<sub>4</sub> **2** showing the atom-numbering scheme.

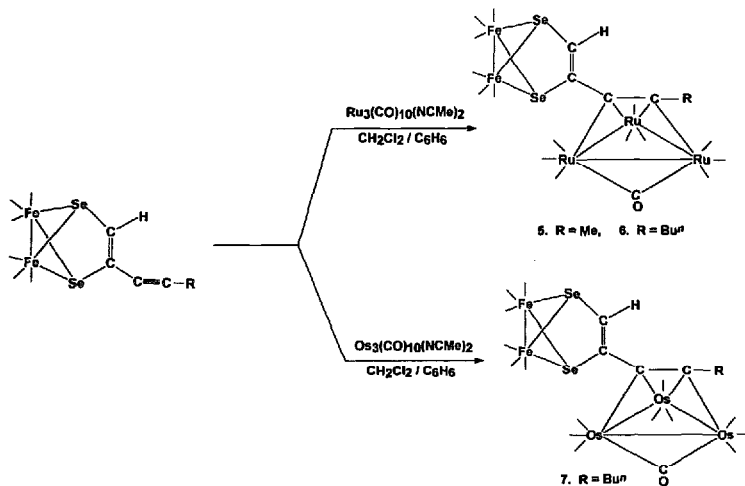
Mo(2)–C(9) (2.205(7) Å), indicating a slight skewness in the bridge. The average C–Mo(1)–Mo(2) angle of 47° is similar to the average C–Mo(2)–Mo(1) angle of 48°.

### 3.3. Synthesis and spectroscopic characterization of $[(CO)_6Fe_2Se_2\{\mu-HC=C(CCR)\}M]$ ( $R = Me, {}^nBu, M = Ru_3(CO)_{10}; R = {}^nBu, M = Os_3(CO)_{10}$ )

Room temperature stirring of benzene solutions containing  $Ru_3(CO)_{10}(NCMe)_2$  with  $[(CO)_6Fe_2\{\mu-SeC(H)=C(C\equiv CR)Se\}]$  ( $R = Me, {}^nBu$ ) afforded  $[(CO)_6Fe_2Se_2\{\mu-HC=C(CCR)Ru_3(CO)_{10}\}]$  (**5**,  $R = Me$ , 43%; **6**,  $R = {}^nBu$ , 40%) (Scheme 2). Similarly, reaction of  $[(CO)_6Fe_2\{\mu-SeC(H)=C(C\equiv C{}^nBu)Se\}]$  with  $Os_3(CO)_{10}(NCMe)_2$  in benzene yielded  $[(CO)_6Fe_2Se_2\{\mu-HC=C(CC{}^nBu)Os_3(CO)_{10}\}]$  (**7**, 38%). Compounds **5–7** were characterized by IR, and  ${}^1H$ ,  ${}^{13}C$  and  ${}^{77}Se$  NMR spectroscopy. The IR spectra of **5** and **6** display almost identical CO stretching patterns in the region 2100–1888  $cm^{-1}$ . The  ${}^1H$  NMR spectrum shows a signal at  $\delta$  6.39 ppm with two pairs of  ${}^{77}Se$  satellites, with H–Se couplings of 55 Hz and 8 Hz, due to short-range and long-range coupling respectively. In addition, it shows a signal for the Me group in **5** and signals for the  ${}^nBu$  group in **6**. The  ${}^{13}C$  ( ${}^1H$ ) NMR spectra of **5** and **6** show a doublet at  $\delta$  120.9 ppm with a C–H coupling of 183 Hz, signals for respective R groups and two signals for each compound in the carbonyl region. The  ${}^{77}Se$  NMR spectra display two signals each for **5** and **6**

with Se–H couplings within the ranges expected for  ${}^2J$  and  ${}^3J$  values. Like the  ${}^{77}Se$  NMR spectra of **1–4**, in **5–7** also, the signal due to the Se atom which is bonded to the CH group is shifted downfield, relative to  $[(CO)_6Fe_2\{\mu-SeC(H)=C(C\equiv CR)Se\}]$  [**11**], by approximately a magnitude of 28–33 ppm. However, in contrast to **1–4**, the signals due to the second Se atom in **5–7** are seen to shift downfield by 18–42 ppm relative to the chemical shift of the corresponding signal in the free diyne complex  $[(CO)_6Fe_2\{\mu-SeC(H)=C(C\equiv CR)Se\}]$  [**11**]. Fig. 2 shows the  ${}^{77}Se$  NMR spectra of  $[(CO)_6Fe_2\{\mu-SeC(H)=C(C\equiv CR)Se\}]$  ( $R = Me$  and  ${}^nBu$ ). It is seen that the downfield signal in each case can be assigned to  $Se(C\equiv CR)$ , on the basis of the multiplet nature of the signal due to coupling of Se with the R groups, a doublet of quartets for  $R = Me$  and doublet of triplets for  $R = {}^nBu$ . In contrast, in **1–7**, the lower field  ${}^{77}Se$  NMR signal occurs as a doublet (Fig. 3), consistent with the removal of conjugation on complexation of metal carbonyl species to the triple bond of  $[(CO)_6Fe_2\{\mu-SeC(H)=C(C\equiv CR)Se\}]$ , and absence of coupling between Se atoms and R groups in  $[(CO)_6Fe_2Se_2\{\mu-C(H)=C(CCR)\}M]$ .

The IR spectrum of  $[(CO)_6Fe_2Se_2\{\mu-HC=C(CC{}^nBu)Os_3(CO)_{10}\}]$ , **7**, in hexane shows a carbonyl stretching pattern in the region 2100–1855  $cm^{-1}$ , similar to that of the previously reported  $[(CO)_6Fe_2Se_2\{\mu-HC=C(CMe)Os_3(CO)_{10}\}]$  [**11**], indicating the presence of bridging CO groups, as well as terminally bonded carbonyl groups. The  ${}^1H$  and  ${}^{13}C$



Scheme 2. Formation of  $[(CO)_6Fe_2Se_2\{\mu-HC=C(CCR)\}M]$  ( $R = Me$  or  ${}^nBu$ ;  $M = Ru_3(CO)_{10}$  or  $Os_3(CO)_{10}$ ).



NMR spectra confirm the presence of  $\text{HC}^t\text{Bu}$  group in 7. The chemical shift of the CH proton is shifted towards higher field by the coordination of the  $\text{Os}_3(\text{CO})_{10}$  group on the substituted acetylenic moiety, whereas the signals for the  $^n\text{Bu}$  group are shifted downfield relative to the chemical shift of the corresponding signal in  $[(\text{CO})_6\text{Fe}_2\{\mu\text{-Se}(\text{H})\text{C}=\text{C}(\text{C}^n\text{Bu})\text{Se}\}]$ .

### 3.4. Molecular structure of $[(\text{CO})_6\text{Fe}_2\text{Se}_2\{\mu\text{-HC}=\text{C}(\text{CCMe})\text{Ru}_3(\text{CO})_{10}\}]$ , 5

Dark red, hexagonal shaped, air-stable crystals of 5 were grown from its dichloromethane–hexane solution at  $-10^\circ\text{C}$  and an X-ray analysis was undertaken. Fig. 4 shows the molecular structure of 5. It can be described as consisting of an  $\text{Fe}_2\text{Se}_2$  butterfly core bridged to the HCC unit of the diyne  $\text{HC}=\text{CC}=\text{CMe}$ , whereas the substituted acetylenic moiety is coordinated in a  $\mu_3\text{-}\eta^2$  mode to a triangular array of ruthenium atoms such that the acetylenic bond is parallel to the  $\text{Ru}(2)\text{-Ru}(3)$  bond of the triangular core. The bond parameters of the  $(\text{CO})_6\text{Fe}_2\text{Se}_2$  unit in 5 are almost identical with those in  $[(\text{CO})_6\text{Fe}_2\{\mu\text{-Se}(\text{H})=\text{C}(\text{C}=\text{CMe})\text{Se}\}]$  [11]. Each Ru atom has three terminal CO groups. The  $\text{Ru}(2)\text{-Ru}(3)$  edge of the triangular core is bridged by a carbonyl group. Overall, the CO groups, bridging-alkyne moiety, and metal–metal bonds define a distorted octahedral geometry around each Ru atom in 5. The metal–metal edge bearing the bridging carbonyl group and  $\sigma$ -bonded to the acetylenic unit forms the longest of

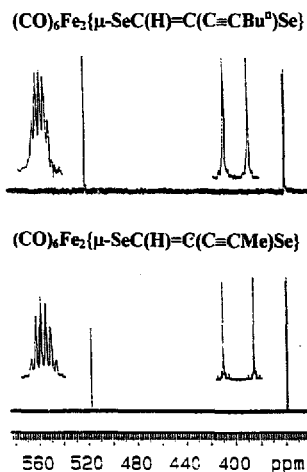


Fig. 2.  $^{77}\text{Se}$  NMR spectra of  $[(\text{CO})_6\text{Fe}_2\{\mu\text{-Se}(\text{H})=\text{C}(\text{CCR})\text{Se}\}]$  ( $\text{R} = \text{Me}$  and  $^n\text{Bu}$ ).

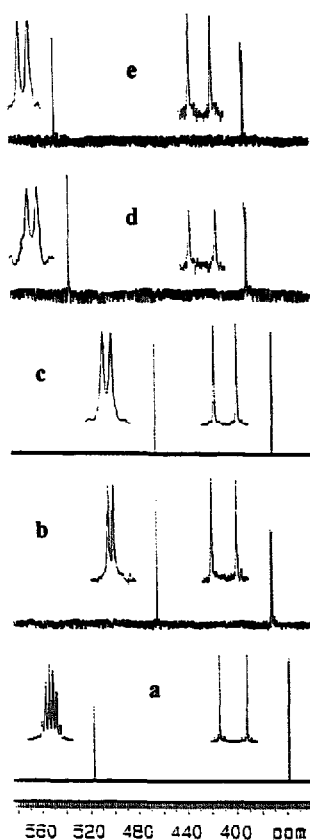


Fig. 3.  $^{77}\text{Se}$  NMR spectra of (a)  $[(\text{CO})_6\text{Fe}_2\{\mu\text{-Se}(\text{H})=\text{C}(\text{C}=\text{CMe})\text{Se}\}]$ , (b)  $[(\text{CO})_6\text{Fe}_2\text{Se}_2\{\mu\text{-HC}=\text{C}(\text{CCMe})\text{Cp}_2\text{Mo}_2(\text{CO})_4\}]$ , (c)  $[(\text{CO})_6\text{Fe}_2\text{Se}_2\{\mu\text{-HC}=\text{C}(\text{CCMe})\text{Co}_2(\text{CO})_6\}]$ , (d)  $[(\text{CO})_6\text{Fe}_2\text{Se}_2\{\mu\text{-HC}=\text{C}(\text{CCMe})\text{Os}_2(\text{CO})_{10}\}]$ , (e)  $[(\text{CO})_6\text{Fe}_2\text{Se}_2\{\mu\text{-HC}=\text{C}(\text{CCMe})\text{Ru}_3(\text{CO})_{10}\}]$ .

the three metal–metal bonds in the  $\text{Ru}_3\text{C}_2$  triangular core, with a  $\text{Ru}(2)\text{-Ru}(3)$  distance of  $2.833(2)\text{ \AA}$ . It is comparable with the  $\text{Ru}\text{-Ru}$  bond distances in related compounds, as in  $(\text{CO})_{10}\text{Ru}_3(\mu_3\text{-}\eta^2\text{-CH}_3\text{CCCH}_3)$  ( $2.8304(7)\text{ \AA}$ ) [25] and in  $(\text{CO})_6\text{Ru}_3(\mu_3\text{-}\eta^1\text{-}\eta^2\text{-}\eta^1\text{-PhCCPh})(\eta^6\text{-C}_{10}\text{H}_8)$  ( $2.8006(13)\text{ \AA}$ ) [26]. The shortest separation between metal atoms in the  $\text{Ru}_3$  triangle is  $2.725(2)\text{ \AA}$ , observed for the  $\text{Ru}(1)\text{-Ru}(3)$  bond. The two  $\text{Ru}\text{-C}\sigma$  bonds,  $\text{Ru}(2)\text{-C}(18) = 2.088(12)\text{ \AA}$  and

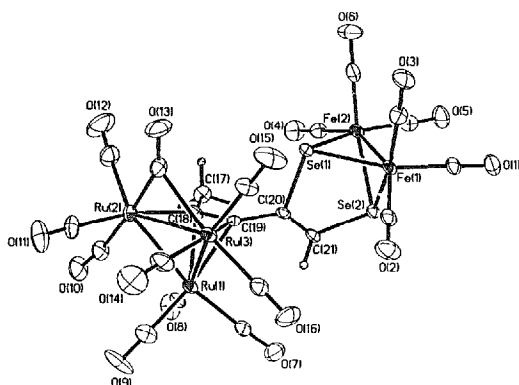


Fig. 4. Molecular structure of  $[\text{Ru}_3(\text{CO})_9]^{2+}$  showing the atom-numbering scheme.

$\text{Ru}(3)-\text{Ru}(19) = 2.111(11) \text{ \AA}$  are shorter than the  $\text{Ru}-\text{C}\pi$ -bonds ( $\text{Ru}(1)-\text{C}(18) = 2.223(12) \text{ \AA}$ ,  $\text{Ru}(1)-\text{C}(19) = 2.258(12) \text{ \AA}$ ), consistent with similar differences observed between  $\text{Ru}-\text{C}\sigma$  and  $\text{Ru}-\text{C}\pi$  bonds in other compounds:  $(\text{CO})_9\text{Ru}_3(\mu_3-\eta^2-\text{CH}_2\text{CCCH}_3)$  (av.  $\text{Ru}-\text{C}\sigma = 2.095(4) \text{ \AA}$ , av.  $\text{Ru}-\text{C}\pi = 2.263(4) \text{ \AA}$ ) [25];  $\{\text{PPN}\}\{(\text{CO})_9\text{Ru}_3(\mu_3-\text{Cl})(\mu_3-\eta^2-\text{PhCCPh})\}$  (av.  $\text{Ru}-\text{C}\sigma = 2.115(6) \text{ \AA}$ , av.  $\text{Ru}-\text{C}\pi = 2.247(7) \text{ \AA}$ ) [25];  $(\text{CO})_9\text{Ru}_3(\mu_3-\text{H})(\mu_3-\eta^2-\text{EtCCEt})(\text{PPh}_3)_2$  (av.  $\text{Ru}-\text{C}\sigma = 2.120(8) \text{ \AA}$ , av.  $\text{Ru}-\text{C}\pi = 2.316(8) \text{ \AA}$ ) [27];  $(\text{CO})_9\text{Ru}_3(\mu_3-\text{H})(\mu_3-\eta^2-\text{EtCCEt})(\text{PPh}_3)_3$  (av.  $\text{Ru}-\text{C}\sigma = 2.118(6) \text{ \AA}$ , av.  $\text{Ru}-\text{C}\pi = 2.300(7) \text{ \AA}$ ) [27] and  $(\text{CO})_9\text{Ru}_3(\mu_3-\eta^1:\eta^2:\eta^2-\eta^1-\text{PhCCPh})(\eta^6-\text{C}_{10}\text{H}_{16})$  (av.  $\text{Ru}-\text{C}\sigma = 2.201(9) \text{ \AA}$ , av.  $\text{Ru}-\text{C}\pi = 2.226(9) \text{ \AA}$ ) [26]. The  $\text{C}(18)-\text{C}(19)$  bond distance of  $1.372(22) \text{ \AA}$  indicates reduction of the free acetylenic bond to an olefinic bond order consistent with the activity of the acetylenic moiety as a formal four electron donor to the triruthenium unit. It is comparable with the corresponding bond distances of the coordinated acetylenic bond in  $(\text{CO})_7\text{Ru}_3(\mu_3-\text{H})(\mu_3-\eta^2-\text{EtCCEt})(\text{PPh}_3)_2$  ( $1.342(11) \text{ \AA}$ ),  $(\text{CO})_9\text{Ru}_3(\mu_3-\text{H})(\mu_3-\eta^2-\text{EtCCEt})(\text{PPh}_3)_3$  ( $1.368(10) \text{ \AA}$ ),  $(\text{CO})_9\text{Ru}_3(\mu_3-\eta^2-\text{CH}_2\text{CCCH}_3)$  ( $1.359(7) \text{ \AA}$ ),  $(\text{CO})_8\text{Ru}_3(\mu_3-\text{H})(\mu_3-\eta^2-\text{CH}_2\text{CC}^i\text{Pr})(\mu_3-\text{PPh}_3)_2$  ( $1.311(6) \text{ \AA}$ ) [28],  $(\text{CO})_8\text{Ru}_3(\mu_3-\text{H})(\mu_3-\eta^2-\text{CC}^i\text{Bu})(\text{PMe}_2\text{Ph})$  ( $1.304(5) \text{ \AA}$ ) [29], but is shorter than the corresponding bond distances in the following compounds:  $(\text{CO})_9\text{Ru}_3(\mu_3-\eta^2-\text{PhCCPh})(\mu_3-\eta^2-\text{Ph}_2\text{PCH}_2\text{PPh}_2)$  ( $1.409(6) \text{ \AA}$ ) [30],  $(\text{CO})_9\text{Ru}_3(\mu_3-\eta^1:\eta^2:\eta^2-\text{PhCCPh})(\eta^6-\text{C}_{10}\text{H}_{16})$  ( $1.409(13) \text{ \AA}$ ),  $(\text{CO})_9\text{Ru}_3(\mu_3-\eta^2-\text{PhCCPh})_2$  ( $1.400(5) \text{ \AA}$ ) [25] and  $\{(\text{CO})_9\text{Ru}_3(\mu_3-\text{Cl})(\mu_3-\eta^2-\text{PhCCPh})\}\{\text{PPN}\}$  ( $1.412(8) \text{ \AA}$ ) [25].

In this paper we have described the facile synthesis of diyne-bridged mixed-metal clusters. Investigations

are in progress to extend the scope of such syntheses to mixed-chalcogenide systems.

#### 4. Supplementary information

Complete tables of atomic coordinates, bond lengths, bond angles, and anisotropic thermal parameters for **2** and **5** (14 pages) are available. Ordering information is given on any current masthead page.

#### Acknowledgements

We thank the Council of Scientific and Industrial Research, Government of India, for financial support. AKD is grateful to CSIR for the award of Senior Research Fellow.

#### References

- (a) K.H. Whitmore, *J. Coord. Chem.*, **17** (1980) 95. (b) L.C. Roof and J.W. Kolis, *Chem. Rev.*, **93** (1993) 1037. (c) P. Mathur, D. Chakrabarty and I.J. Mavunkal, *J. Cluster Sci.*, **4** (1993) 351. (d) P. Mathur, I.J. Mavunkal and A.L. Rheingold, *J. Chem. Soc. Chem. Commun.* (1989) 382. (e) P. Mathur, B. Manimaran, M.M. Hossain, R. Shanbag, J. Murthy, I.S. Saranathan, C.V.V. Satyanarayana and M.M. Bhadbhade, *J. Organomet. Chem.*, **490** (1995) 173.
- (a) P. Mathur, P. Sekar, C.V.V. Satyanarayana and M.F. Mathon, *Organometallics*, **14** (1995) 2115. (b) P. Mathur, D.K. Chakrabarty, Md.M. Hossain, R.S. Rashid, V. Ruginini and A.L. Rheingold, *Inorg. Chem.*, **31** (1992) 1106. (c) P. Mathur, B. Manimaran, Md.M. Hossain, C.V.V. Satyanarayana, V.G. Puranik and S.S. Tavale, *J. Organomet. Chem.*, **493** (1995) 251. [3] (a) P. Mathur, Md.M. Hossain, K. Das and U.C. Sinha, *J.*

- Chem. Soc. Chem. Commun.* (1993) 46. (b) P. Mathur and Md.M. Hossain, *Organometallics*, *12* (1993) 2398.
- [4] (a) D. Seyferth and G.B. Wornack, *Organometallics*, *5* (1986) 2360. (b) T. Fassler, D. Buchholz, G. Huttner and L. Zsolnai, *J. Organomet. Chem.*, *369* (1989) 297.
- [5] P. Mathur, Md.M. Hossain and A.L. Rheingold, *Organometallics*, *12* (1993) 5029.
- [6] (a) A.J. Deeming, M.S.B. Felix, P.A. Bates and M.B. Hursthouse, *J. Chem. Soc. Chem. Commun.*, (1987) 461. (b) J.F. Corrigan, S. Doherty, N.J. Taylor and A.J. Carty, *Organometallics*, *12* (1993) 1365. (c) N.W. Alcock, A.F. Hill, R.P. Melling and A.R. Thompson, *Organometallics*, *12* (1993) 641. (d) J.W. Seyler, W. Weng, Y. Zhou and J.A. Gladysz, *Organometallics*, *12* (1993) 3802.
- [7] N. Pirio, D. Touchard, P.H. Dixneuf, M. Fetouhi and L. Ouahab, *Angew. Chem. Int. Edn. Engl.*, *31* (1992) 651.
- [8] C.J. Adams, M.I. Bruce, E. Horn, B.W. Skelton, E.R.T. Tiekink and A.H. White, *J. Chem. Soc. Dalton Trans.*, (1993) 3313 and references cited therein.
- [9] P. Mathur, A.K. Dash, Md.M. Hossain, C.V.V. Satyanarayana and B. Verghese, *J. Organomet. Chem.*, *506* (1996) 307.
- [10] P. Mathur, Md.M. Hossain, S.N. Datta, R.-K. Kondru and M.M. Bhaubhade, *Organometallics*, *13* (1994) 2532.
- [11] P. Mathur, Md.M. Hossain and A.L. Rheingold, *J. Organomet. Chem.*, *507* (1996) 187.
- [12] D.S. Ginley, R.C. Bock and M.S. Wrighton, *Inorg. Chim. Acta*, *23* (1977) 85.
- [13] G.A. Foulds, B.F.G. Johnson and J. Lewis, *J. Organomet. Chem.*, *296* (1985) 147.
- [14] (a) B.F.G. Johnson, J. Lewis and D.A. Pippard, *J. Chem. Soc. Dalton Trans.*, (1981) 407. (b) P.A. Dawson, B.F.G. Johnson, J. Lewis, J. Puga, P.R. Raithby and M.J. Rosales, *J. Chem. Soc. Dalton Trans.*, (1982) 233.
- [15] G. Sheldrick, Siemens XRD, Madison, WI.
- [16] (a) P. Mathur, A.K. Dash, Md.M. Hossain, S.B. Umbarkar, C.V.V. Satyanarayana, Y.-S. Chen, E.M. Holt, S.N. Rao and M. Soriano, *Organometallics*, *15* (1996) 1356. (b) P. Mathur, Md.M. Hossain, S.B. Umbarkar, C.V.V. Satyanarayana, S.S. Tavale and V.G. Puranik, *Organometallics*, *14* (1995) 959. (c) P. Mathur, A.K. Dash, Md.M. Hossain and C.V.V. Satyanarayana, *J. Organomet. Chem.*, *493* (1995) 257.
- [17] M.R. Churchill and P.R. Bird, *Inorg. Chem.*, *7* (1968) 1545.
- [18] W.I. Bailey, Jr., D.M. Collins and F.A. Cotton, *J. Organomet. Chem.*, *135* (1977) C53.
- [19] W.I. Bailey, Jr., F.A. Cotton, J.D. Jamerson and J.R. Kolb, *J. Organomet. Chem.*, *121* (1976) C23.
- [20] W.I. Bailey, Jr., M.H. Chisholm, F.A. Cotton and L.A. Rankel, *J. Am. Chem. Soc.*, *100* (1978) 5764.
- [21] J.A. Beck, S.A.R. Knox, R.F.D. Stansfield, F.G.A. Stone, M.J. Winter and P. Woodward, *J. Chem. Soc. Dalton Trans.*, (1982) 195.
- [22] A. Mayer, D.J. McCabe and M.D. Curtis, *Organometallics*, *6* (1987) 1491.
- [23] M. Akita, S. Sugimoto, A. Takabuchi, M. Tanaka and Y. Moro-oka, *Organometallics*, *12* (1993) 2925.
- [24] H.E. Amouri, M. Gruselle, Y. Besace, J. Vaissermann, and G. Jaouen, *Organometallics*, *13* (1994) 2244.
- [25] S. Rivomanana, G. Lavigne, N. Lugan and J.-J. Bonnet, *Organometallics*, *10* (1991) 2285.
- [26] A.J. Blake, P.J. Dyson, S.L. Ingham, B.F.G. Johnson and C.M. Martin, *Organometallics*, *14* (1995) 862.
- [27] W. Paw, C.H. Lake, M.R. Churchill and J.B. Keister, *Organometallics*, *14* (1995) 3768.
- [28] D. Nucciarone, N.J. Taylor and A.J. Carty, *Organometallics*, *7* (1988) 127.
- [29] L.J. Farrugia and S.E. Rac, *Organometallics*, *11* (1992) 196.
- [30] S. Rivomanana, G. Lavigne, N. Lugan and J.-J. Bonnet, *Inorg. Chem.*, *30* (1991) 4110.